REPORT DOCUMENTATION PAGE

Form Approved
OMB No. 0704-0188

1. REPORT DATE (DD-MM-YYYY)	2. REPORT TYPE	3. DATES COVERED (From – To)
28032007	Final Technical Report	01 March 2004 – 31 December 2006

4. TITLE AND SUBTITLE
Infrared-Sensitive Photorefractive Polymer Composite Devices

5a. CONTRACT NUMBER

5b. GRANT NUMBER
FA9550-04-1-0096

5c. PROGRAM ELEMENT NUMBER

6. AUTHOR(S)
Professor Nasser N. Peyghambarian

5d. PROJECT NUMBER

5e. TASK NUMBER

5f. WORK UNIT NUMBER

7. PERFORMING ORGANIZATION NAME(S) AND ADDRESS(ES)
Purdue University
Mechanical Engineering Building Room 308
585 Purdue Mall
West Lafayette IN 47907-2088

8. PERFORMING ORGANIZATION REPORT NUMBER

9. SPONSORING/MONITORING AGENCY NAME(S) AND ADDRESS(ES)
Air Force Office of Scientific Research (AFOSR)
875 N. Arlington St., Rm. 3112
Arlington, VA 22203
Dr Charles Lee/NL

10. SPONSOR/MONITOR'S ACRONYM(S)
AFOSR

11. SPONSORING/MONITORING AGENCY REPORT NUMBER
N/A

12. DISTRIBUTION AVAILABILITY STATEMENT
DISTRIBUTION A: Approved for public release. Distribution is unlimited.

AFRL-SR-AR-TR-07-0112

13. SUPPLEMENTARY NOTES

The main goal of the effort was to develop high performing photorefractive (PR) polymer composites working at 1 um by one photon photorefractivity and two photon photorefractive devices operating at 1.5 um. The utilization of these photorefractive devices for beam cleanup and reconstruction of aberrated images was also an important objective of the effort. We have accomplished these goals by developing highly efficient one photon sensitive photorefractive devices operating at about 1 um with high diffraction efficiency, near video rate response time and high two beam coupling gain. This is the first time demonstration of an all-organic photorefractive material beyond 830 nm and the results are the best among any near infrared photorefractive materials under similar experimental conditions.

15. SUBJECT TERMS

16. SECURITY CLASSIFICATION OF:			17. LIMITATION OF ABSTRACT	18. NUMBER OF PAGES	19a. NAME OF RESPONSIBLE PERSON
a. REPORT	b. ABSTRACT	c. THIS PAGE			19b. TELEPONE NUMBER (*Include area code*)
Unclassified	Unclassified	Unclassified	Unclassified	28	(703)

FINAL REPORT

"Infrared-Sensitive Photorefractive Polymer Composite Devices"

SUMMARY OF ACCOMPLISHMENTS

- Successfully developed photorefractive devices sensitive at green (532 nm) and red (633 nm) wavelengths for all-color display applications.
- Demonstrated sub-millisecond writing with high diffraction efficiency using single pulse vibration insensitive hologram writing for updateable 3D display applications.
- Developed highly performing photorefractive devices sensitized at 633 nm which maintain video-rate response time for long exposures.
- Demonstrated acceptable dynamic response of a photorefractive device for aberration correction at very low bias voltages (700V).
- Proved image correction using our polymer devices with an oil-filled phase plate which resemble atmosphere-like turbulence at 633 nm.
- Performed successful experiments and created movies for dynamically corrected images.
- Revealed the application of photorefractive devices for edge detection.
- Extended the sensitization of an all-organic photorefractive device from 830 nm to about 1μm.
- Prepared devices with high diffraction efficiency and near-video rate response time as well as with high two beam coupling gain at 975 nm.
- Successfully developed all-organic photorefractive devices with high diffraction efficiency and near-video rate response time at the telecommunication wavelength of 1550nm by two photon photorefractivity.
- Demonstrated thermal fixing of the holograms and non-destructive readout in photorefractive polymers.
- Non-destructive read-out has been demonstrated at 1550 nm using two photon photorefractive devices.

STATUS OF EFFORT

The main goal of the effort was to develop high performing photorefractive (PR) polymer composites working at 1 μm by one photon photorefractivity and two photon photorefractive devices operating at 1.5 μm. The utilization of these photorefractive devices for beam cleanup and reconstruction of aberrated images was also an important objective of the effort. We have accomplished these goals by developing highly efficient one photon sensitive photorefractive devices operating at about 1 μm with high diffraction efficiency, near video rate response time and high two beam coupling gain. This is the first time demonstration of an all-organic photorefractive material beyond 830 nm and the results are

the best among any near infrared photorefractive materials under similar experimental conditions. Another milestone achieved is the development and demonstration of an efficient photorefractive polymer composite at the important telecommunication wavelength of 1550 nm. The components are optimized to yield more than 40% diffraction efficiency and near video-rate response time. In addition, we have proved that the holograms can be fixed by lowering the temperature of operation and can be read nondestructively. Furthermore, the high voltage required for the working of photorefractive polymer devices is reduced by developing devices with more than 90% internal diffraction efficiency working at voltages as low as 1 kV. This is the first demonstration of any photorefractive polymeric devices with high diffraction efficiency maintaining the video rate response time. We have also successfully performed the image correction experiments at 633 nm using photorefractive composites. An oil-filled phase plate which generates atmospheric-like wavefront aberrations was employed and demonstrated high quality aberration correction using low voltage photorefractive devices. The application of photorefractive devices for edge detection was also identified during the period of report. In order to be used in vibration insensitive applications, we developed polymer composites for single pulse laser operation at 532 nm. With an optimized composite, we demonstrate more than 50% diffraction efficiency using 4 mJ/cm^2 single shot writing and 633 nm continuous wave (cw) beam reading. The present devices showed a 300 μs fast response time. This reveals the potential for these polymer devices in applications which require fast writing and erasure. Since the writing pulse-width is on the nanosecond time scale, the recording is totally insensitive to vibrations. These devices can also be used as a stepping stone to realize all-color holography since they are sensitive to both green (532nm) and red (633nm) wavelengths. The holograms can be written with either of these two wavelengths and can be read by the same wavelength or the other wavelengths with high diffraction efficiency. This demonstrates that these devices have the advantage of performing two-color holography, a step closer to a dynamic full-color holographic recording medium. We have also developed high performing devices sensitive at 845nm with potential applications in image correction.

ACCOMPLISHMENTS / NEW FINDINGS

In photorefractive (PR) materials, a three-dimensional refractive index modulation is induced by a non-uniform illumination. The index modulation is produced as a result of internal space charge-field creation due to selective transport of the photo-generated charges that leads to an internal field-induced index change and thereby to a phase coding of the incident light distribution. The potential applications of PR materials include real time holography, medical imaging, and imaging through scattering media. An interesting application addressed in this report is the beam clean-up in free space communications. Free-space communications currently operate at near visible (~ 850 nm) and near infrared (~ 1550 nm) wavelengths. Even though, several significant advances have been accomplished in developing high performing photorefractive devices, the operating wavelengths of all these devices are limited to less than 850 nm due to the unavailability of a stable photorefractive composite with favorable molecular energetics. Another attractive application of the PR devices is the updateable 3D display applications. We have performed some groundwork experiments for this application too during the period of the report.

We explored the high mobility of TPD (tetraphenyl diphenylamine) molecules and the chemical flexibility of the acrylic chain to develop a new polymer. By the careful manipulation of the orbital energy levels of the components, efficient charge generation, transport and trapping has been achieved in our composites. We have developed new chromophores 3-(N,N-di-n-butylaniline-4-yl)-1-dicyanomethylidene-2-cyclohexene (DBDC) and 3-(4-(azepan-1-yl)-phenyl)-1-dicyanomethylidene-2-cyclohexene (APDC) based on the design strategy for nonlinear molecules. These were prepared to increase the conjugation length and hence the dipole moment of dicyanostyrene-based chromophores, which should lead to an increase in the figure-of-merit. Usually, loading of a single chromophore in a PR composite is limited to less than 40 wt% due to crystallization, but when chromophores are mixed, a higher loading can be achieved without phase separation. Hence, in addition to the samples from a single chromophore (4-homopiperidino benzylidine-malonitrile (7-DCST)), we prepared samples containing two chromophores. Adopting the successful PVK composite recipe, ethyl carbazole (ECZ) was used as the plasticizer and fullerene (C_{60}) was used as the photosensitizer at 633 nm. A new molecule (DBM) was developed as the sensitizer for one photon photorefractivity at 1 μm and two photon photorefractivity at 1.5 μm.

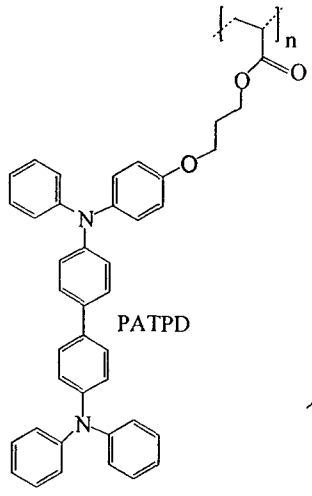

PATPD

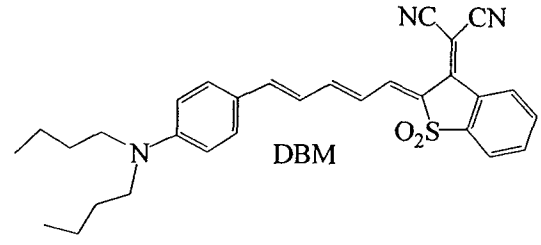

DBM

C_{60}

Charge transport matrix **Sensitizers**

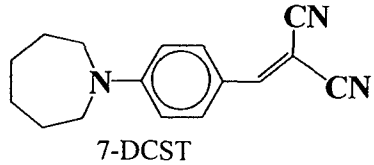

7-DCST

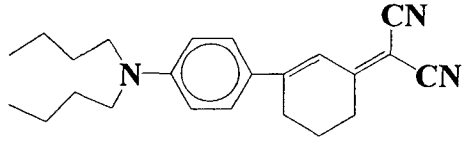

DBDC

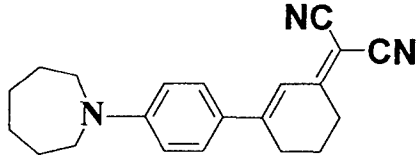

APDC

Nonlinear chromophores

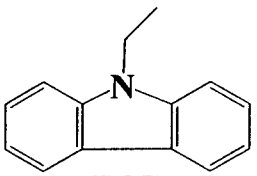

ECZ

Plasticizer

Figure 1. Chemical structure of the components used to make photorefractive composites.

A. PR devices operating at 633 nm

To characterize the PR properties of the samples, four-wave mixing experiments in a standard geometry were performed. Since the overmodulation of diffraction efficiency is a thickness dependent parameter, all PR characterizations were conducted on 105 μm thick samples. The samples were pre-exposed to 4 kJ cm^{-2}. Each sample showed greater than 60% external diffraction efficiency in the steady state. This lowering of external diffraction efficiency from nearly 100% internal may be attributed to absorption to a greater extent (in the DBDC doped samples) and scattering to a smaller extent. Composites prepared included PATPD/7-DCST/ECZ/C_{60} (49.5/35/15/0.5 wt%) (C01), PATPD/DBDC/ECZ/C_{60} (49.5/30/20/0.5 wt%) (C02), and PATPD/7-DCST/DBDC/ECZ/ C_{60} (49.5/20/20/10/0.5) (C03). The photorefractive properties of the composites are summarized in Table 1.

Table 1. Photorefractive properties at 633 nm.

Composites	α [cm^{-1}]	σ_{dark}[a] [pS/cm]	σ_{photo}[a],[b] [pS/cm]	$\eta_{external}$, $E_{\pi/2}$[c] [%],[V/μm]	τ_1, E_{appl} [ms],[V/μm]	Γ[d] [cm^{-1}]
C01	18	5	1500	69, 55	8, 71	150
C02	39	0.01	560	63, 68	16, 81	77
C03	47	0.02	209	58, 40	18, 47	112

[a] At 40 V/μm

[b] At 1 Wcm^{-2}

[c] Applied field to produce overmodulation of the diffraction efficiency.

[d] At 70 V/μm

α – absorption coefficient; σ_{dark}, σ_{photo} – dark and photo conductivities

$\eta_{external}$ – external diffraction efficiency; τ_1 – dominant time constant ; Γ – two beam coupling gain

The most attractive feature of the PATPD-based devices is that they give a stable response for long exposures unlike their PVK counterparts. In PVK-based devices, video rate operation is initially achieved; the response time deteriorates to an unacceptable level after long exposures which limit its use in practical device applications. The reason for the stable response in PATPD-based devices is the absence of chromophores with a highest occupied

molecular orbital (HOMO) above that of the charge transport matrix, whereas in PVK systems the HOMO energy levels of most of the well-optimized chromophores lie above that of PVK. Hence the chromophores act as charge traps in PVK devices whereas such traps are absent in PATPD devices. The absence of chromophore cations is supported by the dynamics of the holographic grating in transient four-wave mixing (TFWM) experiments, where grating build-up and erasure times were recorded as a function of exposure. Illumination conditions were identical to those used to obtain the time constants given in Table 1. From Figure 2, it is clear that video rate response is maintained over the period of exposure, whereas the response time of a similar PVK composite deteriorated several fold.

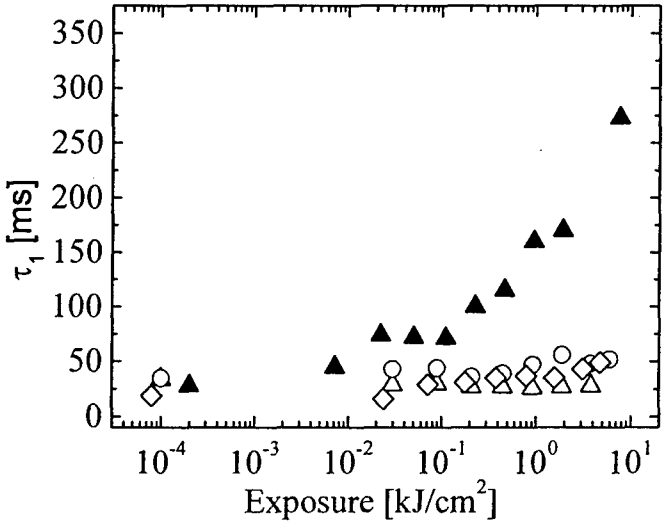

Figure 2 Exposure dependence of the fast time constant of the grating build-up by transient FWM experiments; C01 (triangles), C02 (circles), C03 (diamonds) and a PVK composite (filled triangles) similar to C01 (PVK: 7-DCST: ECZ : C_{60} /49.5 : 35 : 15 : 0.5 wt. %).

These composites showed impressive phase stability, whilst maintaining high diffraction efficiency and gain coefficients compared to other polymer composites previously reported. The exposure history independence of the response time is a significant advance when considering applications where a relatively predictable or a stable response is necessary under continuous exposures. Furthermore, it has been demonstrated for the first time that enhanced diffraction efficiency can be achieved below an applied field of 50 V/μm in a polymeric composite with the video rate response maintained by mixing two chromophores.

B. Devices sensitive at 1μm

We have accomplished a major extension in the sensitivity of the all-organic PR devices into the near-infrared spectral region. Much less consideration has been given to the near-infrared ($\lambda > 830$ nm) region, mainly due to the lack of a composite with favorable PR properties that operates within this spectral range. On the other hand, this wavelength is of major importance, e.g., for beam clean-up, medical imaging and free space optical communications, and compact solid-state lasers operating in this spectral region are readily available. Using our novel photorefractive materials, we demonstrated more than 60% external diffraction efficiency in four-wave mixing experiments, and a fast response time of 33 ms, at an irradiance of 1 W/cm^2. Also, we have developed a composite with very high two

beam coupling gain (> 300 cm^{-1}) at 76 V/μm which is very significant especially for applications where high energy transfer is necessary.

Adopting our experience with high performing photorefractive composite at 633 nm, we prepared several composites to be used at 975 nm. Based on absorption characteristics, phase stability, glass transition temperature, refractive index modulation and photoconductivity, we select a few samples for photorefractive characterization. The selected samples include PATPD/7-DCST/APDC/ ECZ/DBM (39/25/25/10/1) (C04) and PATPD/7-DCST/ECZ/DBM (49/35/15/1 wt. %) (C05).

To characterize the PR properties written in the samples, four-wave mixing experiments were performed in a standard geometry. Two *s*-polarized writing beams, providing a total fluence of 1 W/cm^2 at 975 nm, were incident on the sample with an interbeam angle of 22.5° in air and the surface sample normal tilted 60° with respect to the writing beam bisector. A 3 mW/cm^2 *p*-polarized probe beam counter-propagating along the direction of the closest writing beam to the surface normal was used. The internal diffraction efficiency was calculated as the ratio of the diffracted (I_d) and transmitted (I_t) light intensities ($\eta_{int} = I_d/I_t$). Data points were acquired by continuously increasing the voltage across a 105 μm thick sample. Sample C04 overmodulates the diffraction efficiency at 75 V/μm while C05 overmodulates below 95 V/μm with a diffraction efficiency of about 60%. C04 overmodulates the diffraction efficiency at a lower voltage than C05 because of the higher loading of nonlinear chromophore which is evident from the higher index modulation of C04 from ellipsometry measurements.

In transient four-wave mixing experiments, the sample was biased at a constant voltage under the presence of one writing beam (B2), for a period of 100 ms before the second writing beam (B1) was switched on for a period of 5 s by the use of an electro-optic modulator. After B1 was switched off, the sample remained exposed to B2 for a period of 500 ms before all light was blocked by a mechanical shutter. The dynamics of the grating build-up can be extracted from the following bi-exponential function fit which is correlated to the growth of the space-charge field;

$$\eta(t) = A\sin^2(B(1-e^{-t/\tau_1} - (1-m)e^{-t/\tau_2}), \qquad (1)$$

where η is the diffraction efficiency, A and B constants, τ_1 and τ_2 fast and slow time constants and m a weighting factor, respectively.

The unique nonlocal nature of the PR grating was demonstrated by a two-beam coupling experiment, considered to be a signature of photorefractivity. We adapted the same tilted sample geometry with only *p*-polarized writing beams in a 1:1 ratio providing a total fluence of 1 W/cm^2. The gain coefficient Γ was calculated from (2)

$$\Gamma = \frac{1}{d}[\cos(\alpha_1)\ln(\gamma_1) - \cos(\alpha_2)\ln(\gamma_2)] \qquad (2)$$

where d is the sample thickness, α_1 and α_2 the angles of the two beams with respect to the sample normal inside the PR film, and γ_1 and γ_2 the ratio of each beam's intensity to its intensity in the absence of the other.

Table 2. Photorefractive properties at 975 nm.

Composites	α [cm^{-1}]	σ_{dark}[a] [pS/cm]	σ_{photo}[a] [pS/cm]	Δn[b]	η, $E_{\pi/2}$[c] [%],[V/μm]	τ_1, E_{appl} [ms],[V/μm]	Γ[d] [cm^{-1}]
C04	10	0.06	230	0.012	62, 75	250, 75	300
C05	13	0.1	370	0.0055	65, 95	35, 95	110

[a] At 40 V/μm and 1 Wcm^{-2}

[b] from ellipsometric measurements at 76 V/μm

[c] Applied field to produce overmodulation of the diffraction efficiency.

[d] At 76 V/μm

α – absorption coefficient; σ_{dark}, σ_{photo} – dark and photo conductivities

η – diffraction efficiency; τ_1 – dominant time constant ; Γ – two beam coupling gain

The high-performance novel PR polymer composites at 975 nm have been demonstrated for first time. PR gratings can be written within tens of milliseconds, with high diffraction efficiencies. Furthermore, we have developed a composite with high two-beam coupling of 300 cm^{-1}, one of the best values reported for organic photorefractive materials at any wavelength. The large photoconductivity suggests the possibility of achieving even faster response times within this family of polymer composites. Extending the sensitization of an all-organic PR device to the wavelength of almost 1 μm represents a significant advance in the development of all-organic PR devices for near-infrared imaging and optical communication applications.

C. Photorefractivity at the communication wavelength of 1550 nm

The 1550 nm wavelength is of considerable practical importance as it is orders of magnitude more eye-safe than shorter wavelengths such as 1 μm. Since only very few organic materials undergo electronic transitions required with corresponding optical absorptions at the low energies associated with photons in this wavelength region, we used the two photon absorption (TPA) properties of our successful dye (DBM) at 975 nm. In order to observe photorefractivity under two-photon excitation, the polymer composite should exhibit a nonlinear absorption coefficient of a few cm^{-1} at optical intensities that are below the damage threshold of the sample. For common PR polymer doping levels and at easily achieved short-pulse optical intensities (e.g. GW/cm^2) nonlinear absorption coefficients of the required magnitude result when the TPA cross-section $\delta \sim 50$ GM (Göppert-Mayers) or larger. In addition to the opening of new spectral windows, sensitization through TPA provides the advantage that the material is transparent for any continuous wave (cw) light beam that reads-

out the hologram at the same wavelength. This non-destructive read-out dramatically eases restrictions regarding reading beam intensities and allows for greater film thickness with higher diffraction efficiency. Both features are particularly valuable in imaging applications where high reading intensities and diffraction efficiencies are desired to improve signal-to-noise ratios.

We have identified DBM dye in the polymer composite as an ideal material for generating TPA at 1550 nm. The linear absorption spectrum of the PR polymer composite in the visible and near infrared regions is dominated by a feature centered near 800 nm due to optical absorption by the sensitizer, while no significant linear absorption is seen at wavelengths beyond 1000 nm. Composites prepared include PATPD/7DCST/ECZ/DBM (50/25/15/10) (C06) and PATPD/7-DCST/ECZ/DBM (49/40/10/1 wt. %) (C07). Steady state four-wave-mixing (SSFWM) and two-beam coupling (TBC) experiments were performed to determine the PR characteristics. The experiments were carried out in the standard tilted-sample geometry. A delay line is included in one of the writing beam paths to ensure the temporal overlap of femtosecond pulses inside the polymer sample. Volume holograms were recorded that resemble the interference pattern of two writing beams generated at 1550 nm in an optical parametric amplifier pumped by a femtosecond Ti-sapphire laser. A cw laser diode at 1550 nm was used to probe the grating written in the sample. Figure 3 demonstrates the strong diffraction of cw 1550 nm laser light from the PR grating written in the polymer composite C07 with a time-averaged irradiance (sum of both writing beams) of 40 W/cm^2.

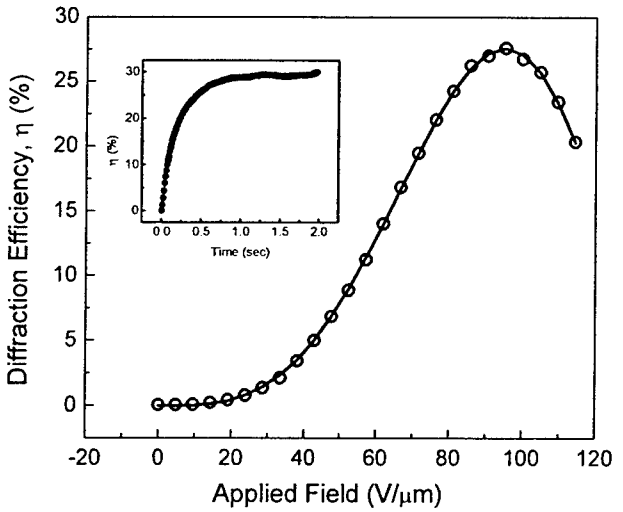

Figure 3. Diffraction efficiency as a function of applied field in a TPA PR sample (C07). Inset shows the growth of the diffracted beam as a second writing beam is turned on at time t=0. Fast response time τ_1 = 40 ms and τ_2 = 270 ms.

We observed 5% and 28% external diffraction efficiency for C06 and C07 respectively, at 98 V/μm. The inset of Fig. 3 shows the growth of the diffracted beam as the second writing beam is turned on at time t = 0 in transient four-wave-mixing (TFWM) experiments. The data agrees well with the biexponential relation describing the fast and slow response times in PR materials. The fast response time so obtained for C07 is 40 ms at 98 V/μm, revealing its potential applications in optical communications where near video rate response times are necessary. TBC experiments performed with this polymer at 1550 nm using a setup similar to

SSFWM without the probe beam revealed net TBC gain greater than 100 cm^{-1} at an applied field of 79 V/μm, confirming the nonlocal nature of the grating formation.

Fine tuning of PR composition

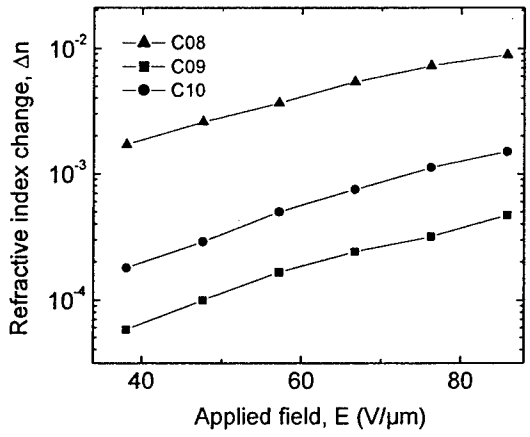

Figure 4. Refractive index change as a function of the applied electric field for composites C08, C09 and C10 measured by steady state ellipsometry at 1550 nm.

In order to improve the PR characteristics of our composites, we have performed ellipsometric measurements to determine the optimum ratio of various functional components. The recipes for the composites were varied to obtain similar T_g around room temperature. The index change obtained at the highest applied fields for the composite PATPD/7-DCST/ECZ/DBM (49:40:10:1 wt. %) (C08) was 9×10^{-3} (Fig.4). For this composite, the refractive index modulation is more than an order of magnitude larger than the composite; PATPD/7-DCST/ECZ/DBM (50:25:15:10 wt. %) (C09). The composite C09 showed an index modulation of 4.5×10^{-4} at the same applied field. The increased non-linear chromophore loading is usually the main reason for the improved index change in polymer composites with similar components and T_g. Interestingly, however, the index change in a composite, PATPD/7-DCST/ECZ/DBM (50:25:20:5 wt. %) (C10), which contained same amount of chromophore (25 wt. %) as C09 but a smaller amount of sensitizer showed an index change of 9×10^{-4} at the same applied field. The reduction of the DBM sensitizer dye loading from 10 wt. % to 5 wt. % has increased the index modulation significantly. Considering that the T_g for these materials are similar, this result indicates that the room temperature orientation of the non-linear chromophore is adversely affected from such a high loading of the sensitizer. This conclusion was further verified by finely tuning the concentration of various components in these composites. As a result of the ellipsometry measurements, an optimized sensitizer concentration of 1 wt. % was used in C08 which provided a maximum index change with fastest response.

In FWM experiment we observed 40% internal diffraction efficiency at an applied electric field of 65 V/μm at 1550 nm. It is clearly seen that the diffraction efficiency

overmodulates at fields exceeding 65 V/μm. The strong diffraction of IR light from this photorefractive thin-film device shows that the nonlinear writing scheme has important potential in holographic applications. Since the absorption of CW light was negligible at this wavelength, the use of the powerful CW reading beams (up to 20 mW) had no effect on the holographic writing/reading/erasure processes in this polymer. In these experiments the grating decay time was independent of the CW reading beam power, in contrast to the case where pulsed reading beams were used. The ease of the restriction in reading beam intensities and non-destructive readout are important advantages in imaging and laser communication applications of photorefractive materials.

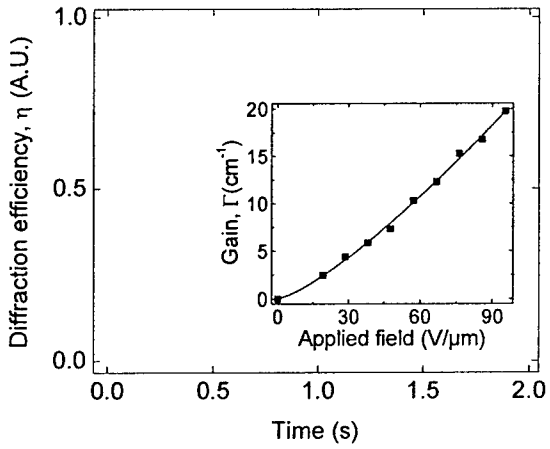

Figure 5. Diffraction efficiency as a function of time for composite C08 showing grating build-up. At time zero the writing beams were turned on. The data fits to the bi-exponential function with a fast time constant (m=0.45) of 35 ms (solid line). Inset: TBC gain as a function of the applied electric field for p-polarized irradiation at 1550 nm. The solid line is a guide to the eye.

A fast response time of 35 ms with a weighing factor of m=0.45 is obtained for C08. The response time is found to be a strong function of the writing beam peak power compared to linearly sensitized photorefractive polymers, showing longer writing times as the writing irradiance was reduced. This suggests that with the incorporation of a sensitizer with larger TPA cross section, the irradiance required to observe near video-rate response times can be brought to smaller writing powers without difficulty. We have also performed two-beam coupling (TBC) measurements using the same pulsed laser at 1550 nm (Figure 5 inset). In these measurements we observed a net gain of 20 cm^{-1} at an applied electric field of 95 V/μm using *p*-polarized irradiation (pulse energy~6 μJ, beam diameter~180 μm). The demonstration of a net TBC gain at 1550 nm proves that the holographic gratings written in these composites are due to the photorefractive effect.

Nondestructive read-out and thermal fixing

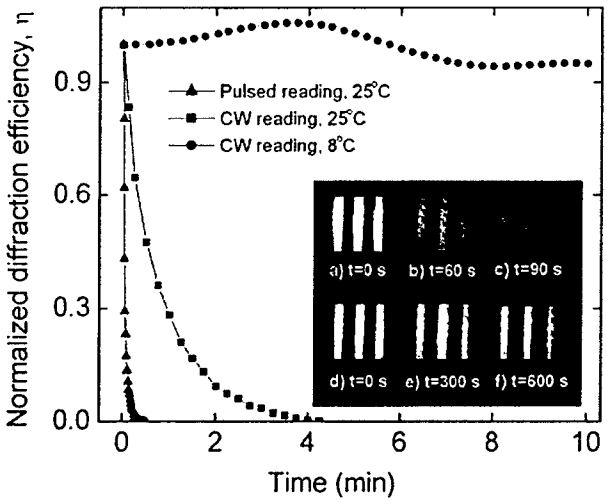

Figure 6. Thermal fixing of the photorefractive hologram and its non-destructive readout. At t = 0, the writing beams are blocked while the powerful (~150W/cm^2) CW reading beam probed the hologram. The decay rate of the gratings is reduced significantly as the temperature is reduced from 25^{0}C to 8^{0}C as a result of NDR and thermal fixing. To demonstrate destructive reading, room temperature reading with a weaker pulsed beam (time-averaged irradiance of 15W/cm^2) is also shown. Inset: Storage of a hologram by thermal fixing at 5^{0}C. At t = 0 the writing beams were blocked and the hologram (vertical bars from a resolution target) was retrieved by the reading beam. Figures from (a) to (c) demonstrate the decay of a non-fixed hologram at room temperature in less than 90s. Retrieval of the fixed hologram (at 5^{0}C) is shown by figures (d) to (f).

Destructive readout (partial erasure of gratings by the reading beam) is one of the main problems to be addressed in photorefractive holographic applications. In many systems where the readout is destructive, the reading beam intensities are kept at very low values, usually less than 1% of the total writing beam intensity, to avoid loss of the data. The use of low power probe beams reduces the signal-to-noise ratio in practical applications. Nondestructive readout (NDR) was demonstrated in photorefractive polymers by use of TPA sensitization. Although NDR allows the use of much more powerful CW reading beams, intrinsic thermal decay still limits the storage time of the photorefractive holograms. To avoid thermal decay and demonstrate true fixing of holograms, we have used a thermal fixing technique and stored the holograms at lower temperatures in our polymer devices after recording them at room temperature. The temperatures of the polymer thin-film devices were reduced from 25°C to around 8°C (using a commercially available low-cost thermo-electric cooler), while the writing beams and electric field were kept on. At 8^{0}C, the writing beams were turned off and the diffraction efficiency was monitored by the 1550 nm CW reading beam with an irradiance of 150 W/cm^2, almost 5 orders of magnitude larger than what was previously used where the readout was destructive. As demonstrated in Figure 6, no significant loss of the diffraction efficiency was observed for many minutes. The holograms could be retrieved after hours with high efficiency. In striking contrast, the PR gratings decayed at a much faster rate at room temperature, being erased completely in a few minutes. By temperature dependent ellipsometry and photoconductivity measurements, the reduced

mobility of the NLO chromophore (7-DCST) and charge carriers (holes) at low temperatures were found to be responsible for the fixing of the holograms. The fixed gratings could be completely erased by increasing the temperature above 15°C and illuminating with one of the pulsed writing beams.

We have recorded two-dimensional images in our polymer thin-film devices and retrieved them several minutes after the writing beams were turned off (Inset to Fig.6). Although some of the edge information was lost because of non-linear writing, the images could be retrieved with relatively good contrast. The holographic images could be retrieved without significant loss after 10 minutes, while the non-fixed holograms at room temperature almost completely decayed in 90 seconds, demonstrating the effectiveness of the combination of thermal-fixing and NDR in applications such as optical data storage.

D. Photorefractive Devices Operating at Low Voltages (633 nm)

High-voltage (5-10 kV) is usually required for the operation of photorefractive polymeric devices, which has been a serious obstacle towards their feasible applications. The ultimate goal is the development of devices that could work with standard DC power supplies such as commercial batteries or line voltages. So far, polymer composites operating near 3kV have been proposed; however the slow response times of seconds have limited their applicability.

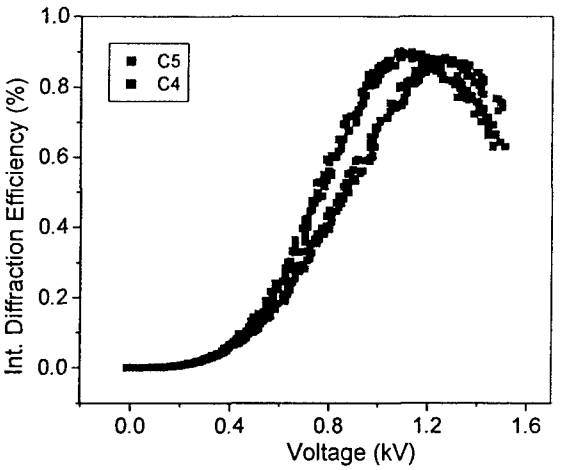

Figure 7. Diffraction efficiency as a function of applied voltage of 20μm thick devices operating at 633 nm; PATPD: DBDC: 7DCST: ECZ: C60 (39.3:40:10:10:0.7) (C4) and PATPD: DBDC: 7DCST: ECZ: C60 (39.5:25:25:10:0.5) (C5).

To measure the strength of the index gratings written in these composites, four-wave mixing (FWM) experiments were performed using s-polarized writing beams and a *p*-polarized reading beam. The measured internal diffraction efficiency is shown in Fig.7. The devices show more than 90% diffraction efficiency with a dominant fast response time of 27ms at 0.9kV. High diffraction efficiency together with video-rate response time at 1 kV is a major advance in the field of organic photorefractive materials. A useful diffraction efficiency

of about 10% can be observed even at a voltage as little as 450V, which demonstrates a major step forward in the feasible applications of photorefractive devices.

Two-color sensitive devices

We have developed new composites which are sensitive both at red and green wavelengths. The composites developed are: PATPD: DBDC: 7DCST: ECZ: C60 (39.3:40:10:10:0.7) (C11) and PATPD: DBDC: 7DCST: ECZ: C60 (39.5:25:25:10:0.5) (C12).

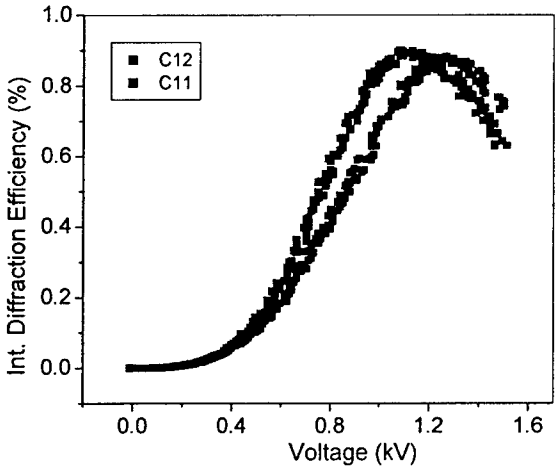

Figure 8. Diffraction efficiency as a function of applied voltage of 20μm thick devices operating at 633 nm.

The results of the two-color recording of the holograms and reading of the recorded holograms with red and green lasers are shown in Fig.8. During reconstruction, each color reads its own grating when read at the proper angle (counter propagating with one of the writing beams). This condition should satisfy Bragg's Law. The red beam can read the green grating if the reading angle is adjusted for Bragg condition at that wavelength ($\sim 5^0$ offset). Similarly, a green beam can read the red grating, too. The devices show more than 90% diffraction efficiency with a dominant fast response time of 27ms at 0.9kV. High diffraction efficiency together with video-rate response time at 1 kV is a major advance in the field of organic photorefractive materials. A useful diffraction efficiency of about 10% can be observed even at a voltage as little as 450V, which demonstrates a major step forward in the feasible applications of photorefractive devices.

E. Pulsed Recording

For single shot pulse experiments, two interfering *s*-polarized beams with a total 4mJ/cm^2 pulse energy and 1ns pulse-width created the grating. A *p*-polarized beam (532nm, DFWM) counter-propagating or a slightly-deviated beam (633nm, NDFWM) probed the efficiency of the grating. The writing beams were incident on the sample with an inter-beam angle of 20° in air and the sample surface was tilted 60° relative to the writing beam bisector resulting in a grating period of 2.6 μm. When a 633nm beam was used for reading, the probe beam was deviated from the counter propagating angle to satisfy the Bragg condition. A red beam is preferred to green for reading, due to lower absorption of the film at longer

wavelengths. A maximum of 56% internal (35% external after all losses) diffraction efficiency was observed. The rise and decay of diffracted signal is depicted in Fig. 9. The reading wavelength was 633nm and the bias field was 95V/μm.

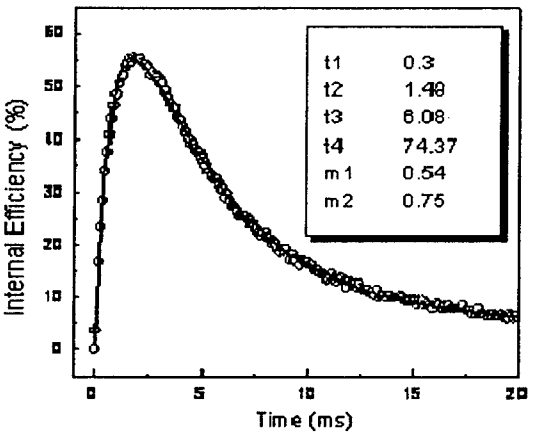

Figure 9. The fast rise and decay of diffraction efficiency when exposed to a single-shot pulse of 1-ns pulsewidth and 4mJ/cm^2 energy. The bias field was kept at 95V/μm and the probe beam wavelength was 633nm. The internal efficiency reached a maximum of 56% (or 35% efficiency after all losses) in only 1.8ms. The fast time constant for the rise is 0.3 ms. This curve can be fitted to an exponential function with 4 time constants (2 for rise and 2 for decay).

The pulse energy defines the number of carriers that can be generated. It should be noted that charge generation is a linear process and therefore the peak power of the pulse is not relevant to photorefractive effect. Pulse energy densities of 4mJ/cm^2 correspond to a total of 1×10^{18} photons/cm^3, half of which are being absorbed. The quantum efficiency as well as the trapping efficiencies will reduce the total density of traps that will create the space-charge field. Varying the pulse energy improves the recording time only very slightly. This point to the fact that the speed is limited by charge carrier mobility and chromophore orientation and not by charge-carrier generation. Both of these processes have more than one time constant associated with them. Since the grating lifetime is short the slow time constants does not contribute much to the performance. Therefore there was no substantial increase in efficiency as we increased the electric field.

Operation of PR devices at 100Hz or higher frame rates requires the decay time to be short so that the information from the previous frame will not overlap with the new frame. The decay of a grating can be accelerated by uniform illumination. Gated cw illumination at 532nm shortly after the writing pulse can erase the grating completely. As shown in Fig. 10, with a gated exposure of 6mJ/cm^2, we were able to erase the grating in a 10ms window. The delay between the writing pulse and uniform gated exposure can be further adjusted for the best signal-to-noise ratio.

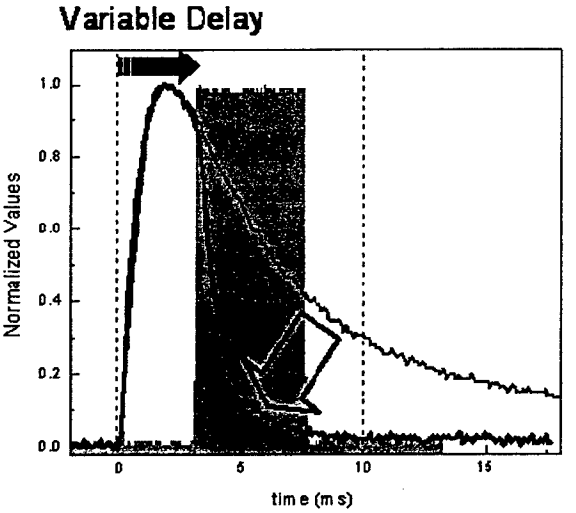

Figure 10. Decay of the single-pulse efficiency is accelerated through a separate, uniform cw illumination at 532nm. The gated illumination lasted only 5ms with an exposure of 6mJ/cm^2. The grating is totally erased 10ms after the pulse arrived. This fast rise and decay proves that we can operate this device at 100Hz (write/erase) frame rates using single pulse writing and gated erasure.

In summary, a single-shot pulse can be used to improve the dynamic response of a photorefractive polymer. Single pulse illumination creates the necessary charge-carriers in a very short time; therefore the speed is limited only by the material's drift mobility and chromophore orientation. We have achieved a response time of 0.3ms through single pulse writing. Notably, grating recording in this case is insensitive to vibrations, which occur on much longer time scales than the writing process. This is an important step towards a vibration insensitive 3D display application.

F. Beam cleanup systems for high-performance laser communication link

Laser communication systems for making connections between earth-, air-, and space-based stations have received worldwide attention in recent years since they possess higher information bandwidth and security than conventional radio-frequency systems. However, when an optical signal is transmitted through a turbulent atmosphere, it will be distorted and the image at the detector will be distorted. As a result, the information capacity will be reduced and the bit error rate will be increased. In order to dynamically correct the errors in the transmitted beam, adaptive optics technology should be used. At the same time, increasingly capable systems are needed to improve image quality when images are collected through the atmosphere or other turbulent media.

Considerable research efforts have been devoted to develop real-time, low-cost adaptive optical systems with high performance. Systems that use nonlinear optical effects such as phase conjugation and multiple-wave mixing as in PR materials are promising candidates for these applications. Various optical systems using photorefractive holograms for real-time wavefront compensation can be designed for communication links depending on the required applications.

System concept

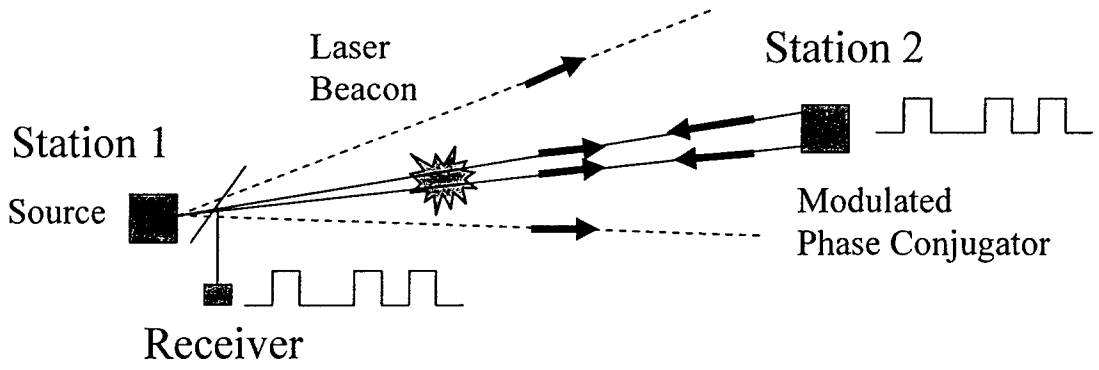

Figure 11. Free-space remote communication link. The task is to transmit temporal signal from the modulated phase conjugation mirror (Station 2) to the source location (Station 1).

The concept of real-time wavefront correction can be understood from the optical communications between two stations viz. Station 1 and Station 2 as shown in Figure 11. The goal is to send optical information from Station 2 to Station 1 through free space. Station 1 has a light source and a receiver, whereas Station 2 has a modulator and phase conjugate mirror. The communication link can be completed in the following steps: (1) Station 1 sends a laser beacon beam to the vicinity of Station 2; (2) when receiving the light from Station 1, Station 2 encodes the signal to be communicated onto the modulator; (3) the encoded beam is redirected to Station 1 using the phase conjugate mirror and detected by the receiver. Although the turbulent atmosphere adds distortion to the beam, Station 1 can always receive the corrected signal from Station 2. In addition, because of the real-time characteristic of the dynamic phase conjugate mirror, even if both stations are mobile, the communication link can still be maintained, enabling its use for dynamic tracking.

To accomplish this link, the system shown in Fig. 12 has been designed and implemented. Experiments have been carried out at 633 nm. As shown in Fig. 12, the beam from a He-Ne laser is vertically (s-) polarized, spatially filtered, and collimated. The collimated beams are split into two arms, the object arm and the reference arm. The reference beam is directed to the PR polymer using a reduction telescope. In the object arm, a Fourier transform lens is introduced and the polymer is placed in the focal plane of the lens. The spectrum of the object beam is overlapped with the reference beam in the polymer and a volume hologram is recorded when the required voltage is applied to the polymer. An aberrator is placed between the lens and the polymer to intentionally distort the beam. In order to obtain the maximum diffraction efficiency, the polymer is aligned in a tilted manner and a p-polarized beam is used to read the hologram. The angle between the two writing beams is 22° and the normal to the sample and the bisector of the two writing beams form an angle of 55°. A quarter waveplate is used to convert the s-polarized beam to the p-polarized beam when the beam double passes it. The reading beam is counter-propagating to the reference beam, generating a phase conjugate object beam. When the phase conjugate object beam passes through the aberrator again, a corrected image is obtained at Station 1.

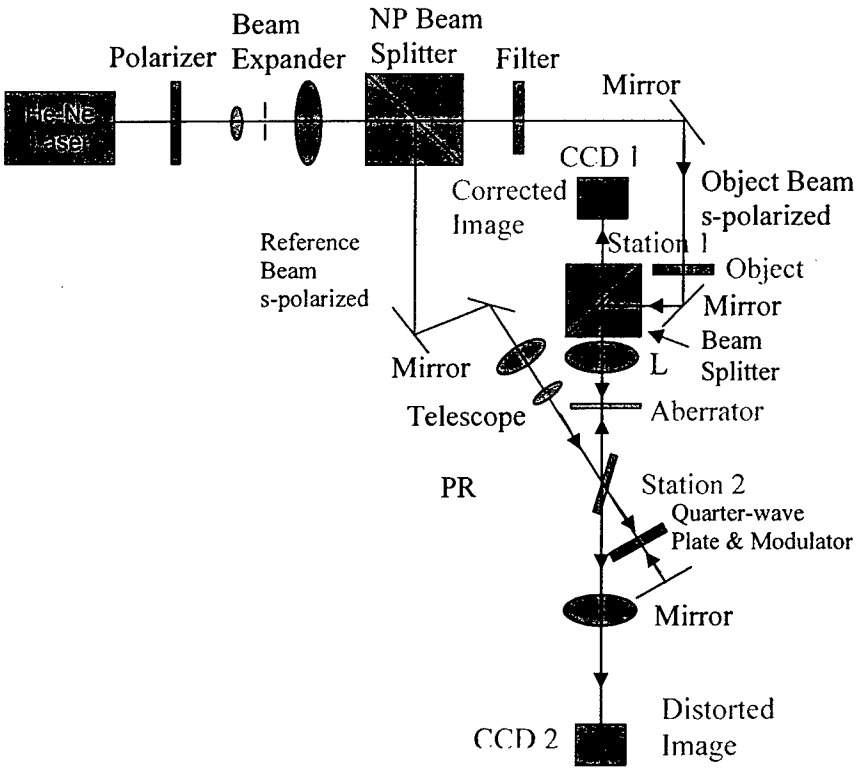

Figure 12. Schematic diagram of the experimental setup beam clean-up.

Since the object beam is imaged to a small area and the reference beam is collimated and has a relatively large area, the system has a large tolerance to misalignment and high information storage density.

(i) Dynamic aberration correction at 633 nm

For dynamic aberration correction, two of the most important performance parameters of the holographic material are response time and diffraction efficiency. A PR polymer composite PATPD: DBDC: ECZ: C60 (49.5:30:20:0.5 wt %) (C13) was used. Video-rate response time can be obtained when the intensity of the writing beams is above 0.5 W/cm^2 in this composite.

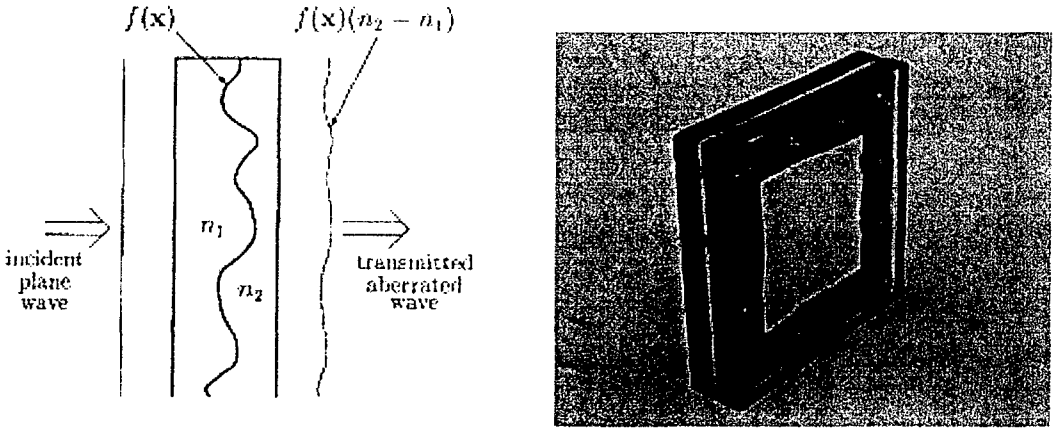

Figure 13. Illustration and photograph of the aberrator.

We have performed a high-quality image correction experiment using an oil-filled phase plate which generates atmospheric-like wavefront aberrations. The aberrator consists of a deformed glass with a refractive index n_1 filled with oil with a refractive index n_2 (Fig. 13). In order to demonstrate dynamic correction of the phase distortion, a stepper-motor is used to move the aberrator continuously in the direction perpendicular to the signal beam propagation. We have successfully performed the experiments and vidoes of dynamically corrected images. Using the oil-filled phase plate, videos were taken when the aberrator was moved at 0.3 mm/s. On the other hand, when the object is moved at the same speed, the corrected images can also be dynamically refreshed without distortions. Figure 14 shows three pairs of distorted and corrected images when the beam carrying the image was transmitted through different positions of the aberrator. From top

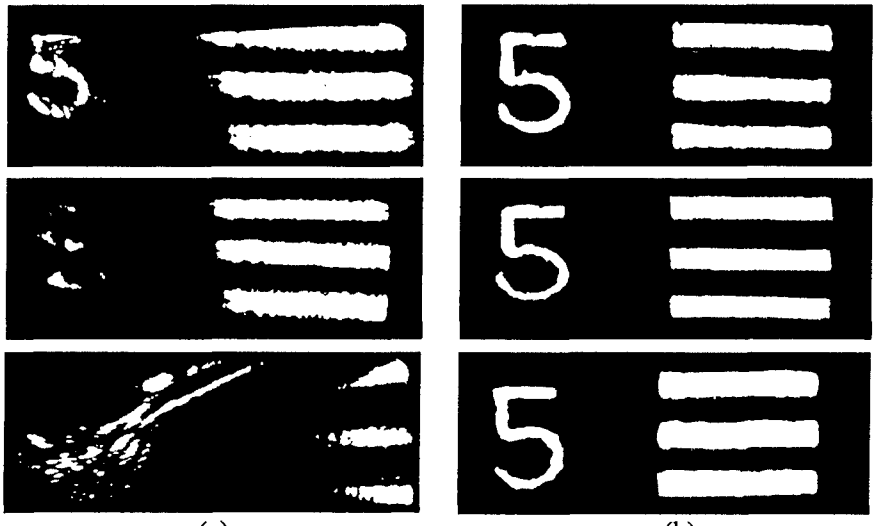

Figure 14. Dynamic correction of atmospheric-like phase distortion when the beam carrying the image transmits through different positions of the aberrator. (a) Distorted images; (b) Corrected images.

to the bottom, the transmitted images were distorted to an increasing extent. The image at the bottom left is severely distorted and the number "5" cannot be recognized at all. It is clearly

seen that in all cases the phase distortion was successfully compensated and the restored images have as high contrast as the images when no aberrator was present.

(ii) Dynamic aberration correction at 633 nm with low working voltages

The above material (C13) shows high diffraction efficiency (100% internal and 60% external) and video-rate response (less than 20 ms) with low power cw laser illumination. Often, the working voltage of photorefractive polymer devices is higher than 6 kV. For many applications that require real-time processing, it is very desirable to reduce the working voltage while maintaining other photorefractive properties. Recently, we achieved this by carefully engineering the thickness of the sample and developing new samples with lower over-modulation voltage.

For comparison, the steady-state field-dependent diffraction efficiencies for materials with thicknesses of 105 μm, 53 μm, and 20 μm are shown Fig. 15 (a)-(c) respectively. It can be seen that for 20 μm and 53 μm samples, the index gratings are not overmodulated, but they indeed provide required efficiencies for optical information processing. A comparison of these samples with various thicknesses is shown in Table 3.

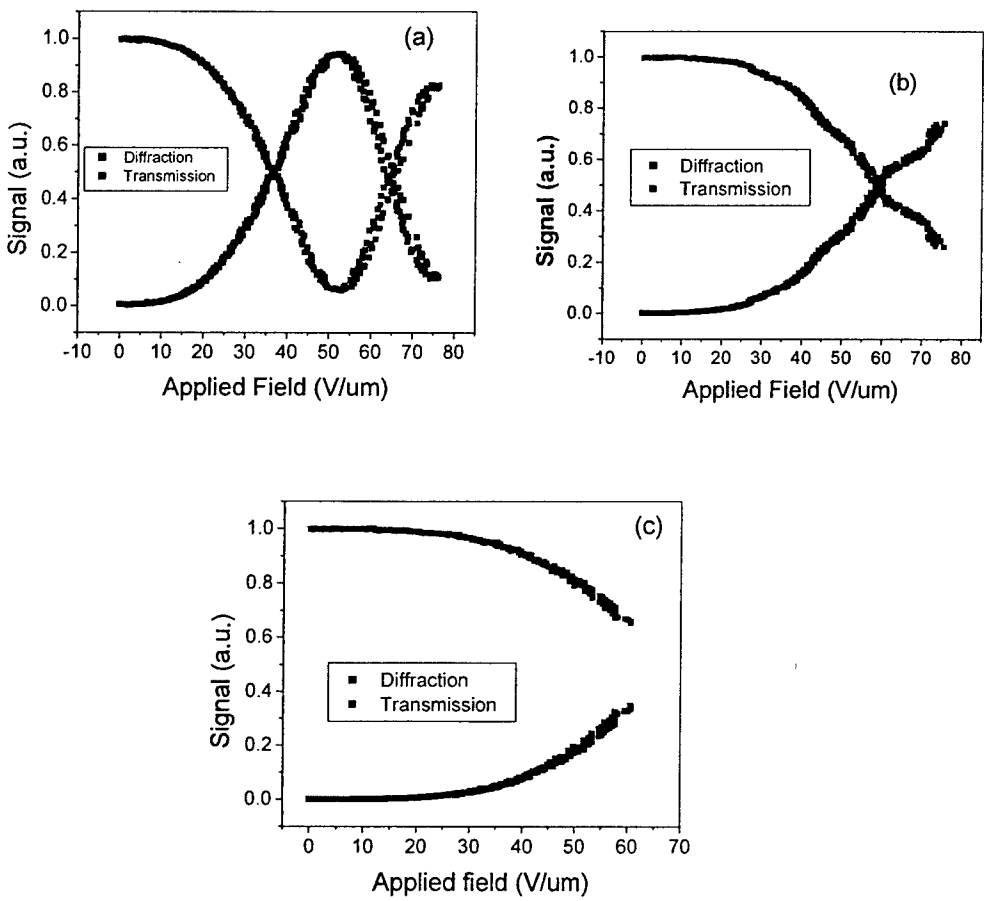

Figure 15. Diffraction efficiencies of the samples with various thicknesses. (a) 105 μm; (b) 53 μm; (c) 20 μm.

Thickness of the sample (μm)	Voltage/device	Diffraction efficiency
105	5.5 kV	94%
53	4 kV	74%
20	1.2 kV	35%

Table 3. A comparison of the sample thickness with applied voltage per device and diffraction efficiencies.

Using 20-μm devices, we have successfully performed dynamic correction of atmospheric-like phase distortion when the aberrator was moved at 0.3 mm/s. The image quality is as good as that using 105-μm samples requiring 6 kV.

In order to further reduce the working voltage, two new PR samples with lower overmodulation voltage values were used. The composition of the devices are PATPD: RLC:7DCST:ECZ:C60(39.3:40:10:10:0.7wt%) (C14), and PATPD:APDC:7DCST:ECZ:C60 (39.5:25:25:10:0.5 wt%) (C15).

For dynamic aberration correction, when the aberrator was moved at 0.3 mm/s, the working voltage for C14 is about 800V and that for sample C15 is about 600-700 V. Both samples have a thickness of 20-μm. Figure 16 shows the corrected images using C15 at different applied voltages. The applied voltages for Fig. 16 (a) – (d) are 700V, 600V, 500V, and 400V, respectively. When the applied voltage was decreased, the diffraction efficiency dropped and the intensity of the diffracted image was lower. It can be seen that the working voltage has been significantly reduced using 20-μm samples while the image quality remains the same. (The movies have been provided to the program officer).

(a) (b)

(c) (d)

Figure 16. Corrected images using sample 3 at different voltages. (a) 700V; (b) 600V; (c) 500V, and (d) 400V.

In order to further reduce the working voltage, we tried two approaches. One is to reduce the thickness of the previous sample and the other is to use a different material with a lower saturation voltage. Figure 17 compares the transient response of the previous sample with 53-μm thickness to that of a 20-μm thick sample. The applied voltages were 3 kV and 1.1 kV, respectively. With the reduced thickness and the applied voltage, the diffracted signal strength decreases nonlinearly, but it is still strong enough to record good movies with dynamic correction of the distorted phase.

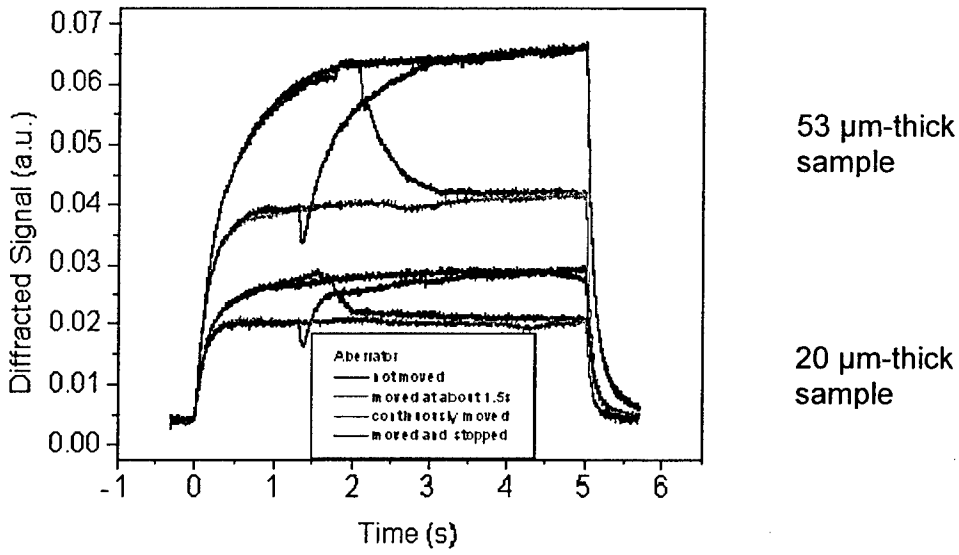

Figure 17. Dynamic response of the system using the above material with different thickness.

A new material composition with a low saturation voltage is PATPD:APDC:7DCST:ECZ:C60 (39.5:25:25:10:0.5 wt%) (C16). Although this material has high absorption when 105-μm thick devices were used, it works well with 20-μm thick devices under an applied voltage of 700 V. Figure 18 demonstrates the transient responses of the system using this material when the aberrator was static and moved at 0.3 mm/s. Figure 19 shows the variation of the dynamic responses of the system when the aberrator was moved

at different speeds. As shown in the Figure 19, even when the aberrator was moved at 1.0 mm/s, good diffracted signal can still be obtained.

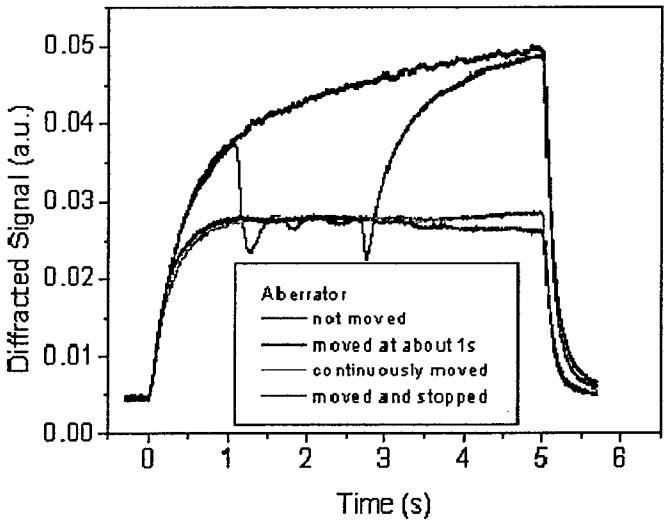

Figure 18. Dynamic response of the system using the 20-μm thick composites PATPD:APDC:7DCST:ECZ:C60 (39.5:25:25:10:0.5 wt%) with 700V voltage applied.

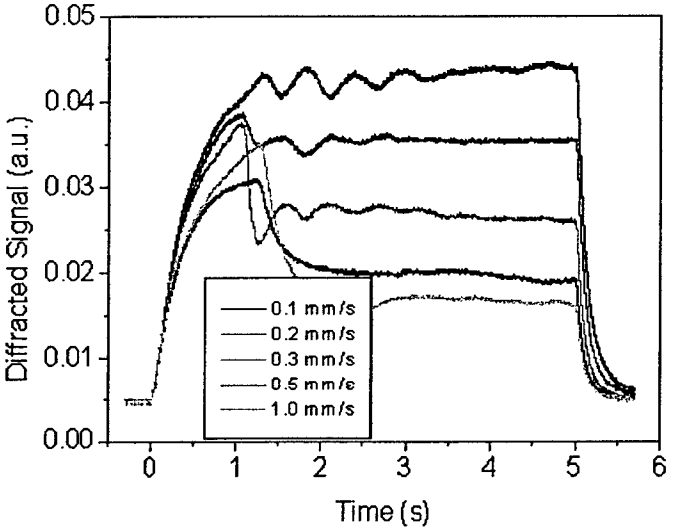

Figure 19. Dynamic response of the system at 700V for different aberrator speeds.

The dependence of the intensity of the diffracted light on the intensity of the object beam is shown in Fig. 20. As seen from this figure, when the intensity of the reference beam is fixed, the diffracted signal increases with an increase in the object beam power.

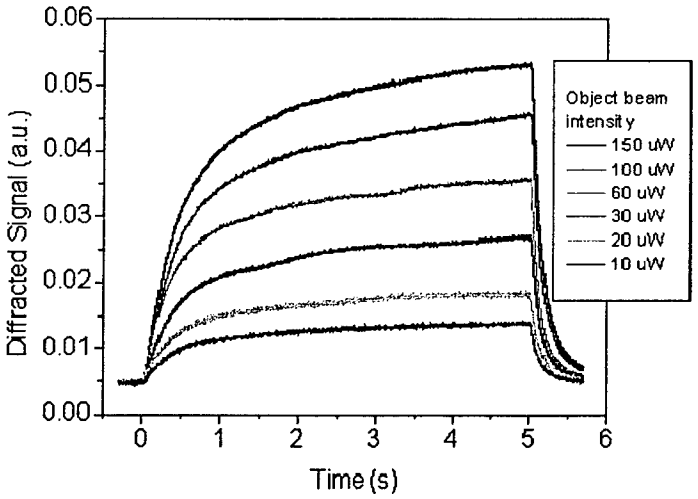

Figure 20. Dynamic response of the system at 700V as the object beam intensity varies.

In summary, we have performed a quantitative study of the dynamic responses of the aberration correction system under various conditions. A system for comparing the diffracted signal when the aberrator is static with that when the aberrator is moved at different speeds has been implemented. The diffracted signal decreases monotonically as the speed of the aberrator is increased. The diffracted signal has been studied as a function of the object beam intensity and the external applied field. To further reduce the working voltage, we tried to reduce the thickness of the sample and also used a different material with a lower saturation voltage. Measurements of the dynamic response of the system under these conditions have also been performed.

G. Edge detection

Edge detection can also be performed with the same set-up by adjusting the sample position and intensity ratio of the two writing beams. Edge enhancement can be treated as a high-pass spatial filtering operation. It can be implemented with a matched filter correlator by blocking the low frequency components in the Fourier plane. However, it requires accurate alignment of the spatial filter and is not energy efficient. We demonstrate that our system overcomes this problem and can be used to perform edge-enhanced image processing easily by exploiting the nonlinearity inherent in PR polymer. In our system, the intensity interference pattern is formed by the spatial Fourier transform of the object and the collimated reference beam. The strength of the local grating and hence the diffraction efficiency is proportional to the modulation depth, which is a function of the intensity values of the signal and reference beams when the intensity of the reading beam is much weaker. Inside the sample, the center of the signal beam corresponds to the object information of lower frequency and contains most of the signal energy, while the wings of the diffracted pattern corresponds to the high frequency information of the object and contains less energy. Therefore, if the intensity of the object beam is adjusted so that the intensity of the high-frequency signal is comparable to that of the reference beam and the intensity of the low-frequency signal is much greater than that of the reference beam, the local grating generated by the former two beams will possess high efficiency and the local grating generated by the

latter two beams will possess low diffraction efficiency. Since the low-frequency signal is attenuated and the high-frequency signal is well reconstructed, the edge enhancement can be realized. In this application, the total intensity of the object beam is usually much higher than that of the reference beam at the Fourier transform plane. Impressive experimental results have been accomplished. The processed images have a high contrast and the edge-enhancement efficiency is close to unity. This technique enables us to select the object features of particular frequencies by adjusting the intensities of the writing beams.

H. Molecules with Strong Two-photon Absorption in the Telecommunications Band

(Report from Prof. Seth R. Marder)

In designing chromophores for two-photon absorption (2PA) in the near-IR telcommunications wavelength range, we have chosen to focus on dipolar donor-acceptor chromophores. Firstly, in this class of chromophores, there is no symmetry restriction on the states into which 2PA may occur and so 2PA into the one-photon allowed state may be observed; i.e. 2PA can take place at half the 1PA photon energy. In contrast, in the case of quadrupolar chromophores, 2PA and 1PA selection rules are mutually exclusive, which often means the lowest energy 2PA is seen at a photon energy significantly greater than half that of the 1PA maximum. Secondly, dipolar chromophores often have rather low-energy charge-transfer-type transitions and are thus good candidates for achieving 2PA well into the near-IR region. Accordingly, we have reported a non-degenerate pump-probe value of δ = ca. 1500 GM for a dipolar chromophore.[1] Quantum-chemical calculations suggest that the value for degenerate 2PA is significantly (ca. 40%) lower than the non-degenerate value, but still large. The transition energy corresponding to two 1.44 μm photons and, as expected for a strongly dipolar chromophore, this corresponds to the same state accessed by 1PA.

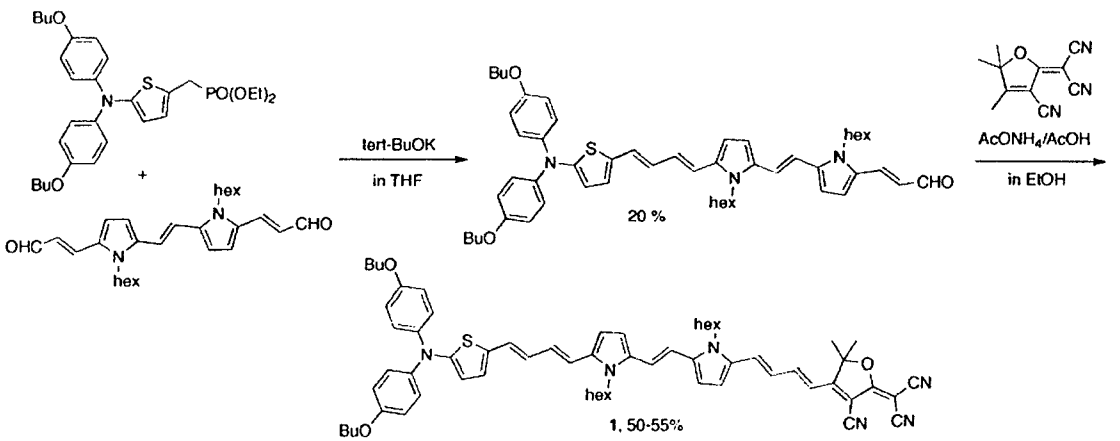

Figure 1. Synthesis of an extended dipolar chromophore, **1**.

[1] Beverina, L.; Fu, J.; Leclercq, A.; Zojer, E.; Pacher, P.; Barlow, S.; Stryland, E. W. V.; Hagan, D. J.; Brédas, J.-L.; Marder, S. R., *J. Am. Chem. Soc.* **2005**, *127*, 7282.

We have recently synthesized a related chromophore, **1**, as shown in Figure 1. As shown in Figure 2, the main low-energy 1PA is at 1.47 eV, corresponding to a photon wavelength of 845 nm; thus, one would anticipate the possibility of a 2PA peak at 1690 nm, rather too far to the red for our current needs. However, as also shown in Figure 2, there is rather strong 2PA into a higher lying state (or states) with a peak cross-section of almost 3000 GM just outside our region of interest. However, the cross-section is still very large (2540 ± 20%) at 1.3 μm, with reasonably strong 2PA (δ > 500 GM) throughout the entire telecom band. Cyclic voltammetry of this chromophore reveals a reversible molecular oxidation at –0.22 V vs. ferrocenium / ferrocene, whereas there is a less reversible reduction at –1.13 V.

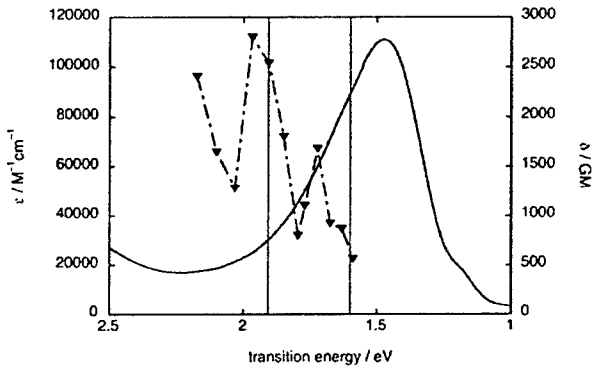

Figure 2. One-photon (solid line) and degenerate two-photon (symbols and broken line, acquired with Z-scan) solution spectra for compound **1** plotted vs. transition energy. The vertical lines denote the transition energies corresponding to 2PA of 1.3 (left) and 1.55 μm (right) photons.

We have also synthesized the chromophore **2**, shown in Figure 3, as part of further our understanding of structure-property relationships in this class of molecules. As expected from the less extensive conjugation vs. **1**, the 1PA absorption maximum is considerably blue-shifted; in fact it is at ca. 750 nm, suggesting the possibility of strong 2PA at 1.5 μm. Whether strong 2PA is indeed seen into the low-energy 1PA state (as was the case for the chromophores in Ref 1), or whether there is stronger absorption into higher lying states (as in the case of **1**), is the subject of ongoing 2PA measurements.

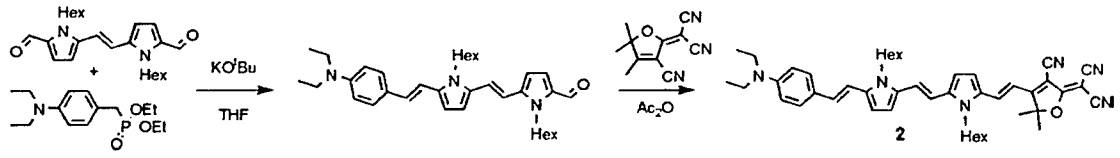

Figure 3. Synthesis of a new chromophore with shorter conjugation than **1**.

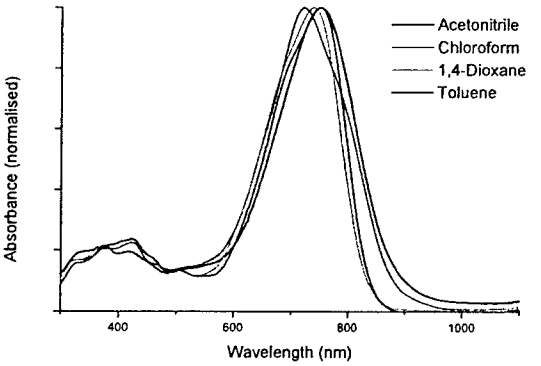

Figure 4. 1PA spectra of **2** in various solvents.

PERSONNEL SUPPORTED:

Nasser Peyghambarian, PI
Jayan Thomas, Assistant Research Professor
Seth R. Marder, Professor
Muhsin Eralp, Graduate Student
Savas Tay, Graduate Student
Lirong Wang, Graduate Student

PUBLICATIONS:

1. "Bis-triarylamine polymer-based composites for photorefractive applications," J. Thomas, C. Fuentes-Hernandez, M. Yamamoto, K. Cammack, K. Matsumoto, G. A. Walker, S. Barlow, B. Kippelen, G. Meredith, S. R. Marder, N. Peyghambarian, *Adv. Mater.* **16**, 2032 (2004).
2. "Video-rate compatible photorefractive polymers with stable dynamic properties under continuous operation," C. Fuentes-Hernandez, J. Thomas, R. Termine, M. Eralp, M. Yamamoto, K. Cammack, K. Matsumoto, G. Meredith, N. Peyghambarian, B. Kippelen, G. A. Walker, S. Barlow, S. R. Marder, *Appl. Phys. Lett.* **85**, 4561 (2004).
3. "High-performance photorefractive polymer operating at 975nm wavelength," M. Eralp, J. Thomas, S.Tay, G. Li, G. Meredith, A. Schülzgen, N. Peyghambarian, G. A. Walker, S. Barlow, S. R. Marder, *Appl. Phys. Lett.* **84**, 1095 (2004).
4. "Dynamic correction of a distorted image using a photorefractive polymer composite," J. G. Winiarz, F. Ghebremichael, J. Thomas, G. Meredith, N. Peyghambarian, *Opt. Exp.* **12**, 2517 (2004).
5. "Photorefractive polymer operating at the optical communication wavelength of 1550 nm," S. Tay, J. Thomas, M. Eralp, G. Li, B. Kippelen, S. R. Marder, G. Meredith, A. Schülzgen, N. Peyghambarian, *Appl. Phys. Lett.* **85**, 4561 (2004).
6. "All-optical dynamic correction of distorted communications signals using a photorefractive polymeric hologram," G. Li, M. Eralp, J. Thomas, S.Tay, A. Schülzgen, N. Peyghambarian, *Appl. Phys. Lett.* **86**, 161103 (2005).

7. "Organic Optoelectronics" *N. Peyghambarian and R. A. Norwood Optics & Photonics News* April 2005, 28.
8. "High-performance photorefractive polymer operating at 1550 nm with near-video-rate response time," S. Tay, J. Thomas, M. Eralp, G. Li, R. A. Norwood, A. Schülzgen, M. Yamamoto, S. Barlow, G. A. Walker, S. R. Marder, and N. Peyghambarian, *Appl. Phys. Lett.* **87**, 171105 (2005).
9. "Photorefractive Polymers with Superior Performance," J. Thomas, M. Eralp, S. Tay, G. Li, M. Yamamoto, R. Norwood, S. R. Marder and N. Peyghambarian, *Optics and Photonics News* (special edition on "Optics in 2005"), December 2005, Page 31.
10. "Photorefractive polymer device with video-rate response time operating at low voltages," M. Eralp, J. Thomas, G. Li, S. Tay, A. Schülzgen, R. A. Norwood, and N. Peyghambarian and M. Yamamoto, *Opt. Lett.* **31**, 1408 (2006).
11. "Submillisecond response of a photorefractive polymer under single nanosecond pulse exposure",M. Eralp, J. Thomas, S. Tay, G. Li, A. Schülzgen, R. A. Norwood M. Yamamoto and N. Peyghambarian, *Appl. Phys. Lett. **89**,* 114105 (2006).

Book Chapter

J. Thomas, R. A. Norwood and N. Peyghambarian, *"New Directions in Holography and Speckles,"* editors: H. J. Caulfield and C. S. Vikram, American Scientific Publishers, California (with the publisher).

INTERACTIONS/TRANSITIONS

Transition to Industry

Our research results were transitioned to a company in San Diego area, Nitto Denko Technical. This company is preparing devices for ultimate commercial use. They have also been able to make larger size devices, the largest being 10 cm2, to date. Fabrication of even larger samples of 4" x 4" is underway.

a) Participation/presentations at meetings, conferences, seminars etc.

"Nonlinear absorption sensitization of a photorefractive polymer composite for operation at 1.55 microns," N. Peyghambarian, S. Tay, J. Thomas, M. Eralp, G. Li, G. Meredith, A. Schülzgen, and S. R. Marder, Presented at the Nonlinear Optics: Materials, Fundamentals and Applications Conference, Waikoloa, HI, August 2-6, 2004.

"Near Infrared photorefractive polymer composites with high diffraction efficiency and fast response time," J. Thomas, M. Eralp, S. Tay, G. Li, S. R. Marder, G. Meredith, R. A. Norwood, A. Schülzgen, and N. Peyghambarian, SPIE International Symposium, SPIE's 49th Annual Meeting, Optical Science and Technology 2 - 6 August 2004, Denver, Colorado USA.

"Novel Infra-red Sensitive Photorefractive Polymer Composite," S. Tay, J. Thomas, M. Eralp, G. Li, B. Kippelen, S. Marder, G. Meredith, A. Schulzgen and N. Peyghambarian, 2004 CLEO/IQEC, 2004, San Francisco, CA.

"Photorefractive polymer operating at 1550nm with 40% diffraction efficiency and 35ms response time," (Invited talk) S. Tay, J. Thomas, M. Eralp, G. Li, J. Winiarz, A. Schülzgen, R. A. Norwood S. R. Marder, and N. Peyghambarian, SPIE Annual Meeting, San Diego, July 31-August 4, 2005.

"Photorefractive adaptive optics for dynamic correction of atmospheric-like wavefront aberrations," G. Li , J. Thomas, M. Eralp, S. Tay, J. Winiarz, A. Shülzgen, R. Norwood, and N. Peyghambarian, SPIE Annual Meeting, San Diego, July 31-August 4 2005.

"Breakthroughs in Photorefractive Polymers," Peyghambarian, N., Presented at the AFOSR Polymer Chemistry and Polymer Matrix Composites Program Reviews, San Diego, CA, August 8-12, 2005.

"Photorefractive polymer devices operating at practical voltages" (Invited talk), M. Eralp, J. Thomas, G. Li, J. Winiarz, S. Tay, A. Schülzgen, R. A. Norwood and N. Peyghambarian, Frontiers in Optics, OSA Annual Meeting, Tucson, October 16-20,2005.

"Recent Advances in Two Photon Photorefractive Polymers", J. Thomas, S. Tay, M. Eralp, J. Winiarz, G. Li, S. R. Marder, A. Schülzgen, R. A. Norwood and N. Peyghambarian, Frontiers in Optics, OSA Annual Meeting, Tucson, October 16-20, 2005.

"Photorefractive polymers with sub-millisecond response time", J. Thomas, M. Eralp, S. Tay, G. Li, P. Wang, M.Yamamoto, A. Schülzgen, R. A. Norwood and N. Peyghambarian, Optics and Photonics, SPIE Annual Meeting, San Diego, 13-17 August 2006.

"Photorefractive polymer in reflection geometry with large efficiency, M. Erlap, J. Thomas, S. Tay, G. Li, R. A. Norwood, N. Peyghambarian, Optics and Photonics, SPIE Annual Meeting, San Diego, 13-17 August 2006.

"Efficient local fixing of photorefractive polymer holograms recorded with CW and pulsed beams" *(Invited Paper)*, G. Li, M. Eralp, P. Wang, J. Thomas, S. Tay, R. A. Norwood, M. Yamamoto, N. Peyghambarian, Optics and Photonics, SPIE Annual Meeting, San Diego, 13-17 August 2006.